


Experimental Study of the Source of CO Anomalies in Mines Based on Microscopic Changes

Jiuling Zhang^{1,2}, Gaoyang Ruan^{1,2,*}  and Jianguang Chen^{1,2}

¹ School of Mining Engineering, North China University of Science and Technology, Tangshan 063000, China; ninety2000@163.com (J.Z.); cjg2827132399@163.com (J.C.)

² Hebei Province Key Laboratory of Mine Development and Safety Technology, Tangshan 063000, China

* Correspondence: ruangaoyang2022@163.com; Tel.: +86-18325593661

Abstract: The phenomenon of abnormal CO emergence occurred in a working face of Tangshan mine, and the CO source was analyzed from the two perspectives of CO detection method optimization and microstructure changes in the low-temperature environment of the coal body. Then, the critical index system was optimized. The CO identification tube test results and gas chromatograph test results are combined to derive a fitting formula, and the CO identification tube test results are used as the independent variable to obtain the gas chromatograph test results, which can effectively eliminate the error of small CO identification tube test results. The analysis of raw coal and coal samples heated by water bath at 30 °C, 40 °C, and 50 °C was carried out using low temperature liquid nitrogen adsorption and thermogravimetric and infrared spectroscopy experiments. It was found that the pore structure of the coal body developed as the temperature increased; the oxidation reaction occurred in the low-temperature state when heat was absorbed to produce CO. The thermal decomposition of carbonyl group was found to be the main source of CO. Finally, the index of spontaneous combustion of coal is optimized according to the temperature, and the index systems represented by $O_2/(CO_2+CO)$, CH_4 and CO_2/CO were determined from 30~80 °C, 90~180 °C and 18~240 °C, respectively.

Keywords: CO source; free radical reaction; CO identification tube; optimization of self-ignition index



Citation: Zhang, J.; Ruan, G.; Chen, J. Experimental Study of the Source of CO Anomalies in Mines Based on Microscopic Changes. *Fire* **2022**, *5*, 57. <https://doi.org/10.3390/fire5030057>

Academic Editors: Haiyan Wang, Feng Li, Huiyong Niu, Minbo Zhang and Xuyao Qi

Received: 4 March 2022

Accepted: 21 April 2022

Published: 25 April 2022

Publisher's Note: MDPI stays neutral with regard to jurisdictional claims in published maps and institutional affiliations.



Copyright: © 2022 by the authors. Licensee MDPI, Basel, Switzerland. This article is an open access article distributed under the terms and conditions of the Creative Commons Attribution (CC BY) license (<https://creativecommons.org/licenses/by/4.0/>).

1. Introduction

With the joint efforts of many scholars at home and abroad, mine accidents in China have shown a general downward trend in recent years, but still face problems such as complex coal mining conditions and serious mine fire threats [1,2]. In Tangshan mine 0291 coal seam, CO content was detected to exceed the limit during coal mine production; however, spontaneous coal combustion is not the only source of underground CO [3], and it is a serious threat to mine safety management since CO is mostly used as an indicator gas for early spontaneous combustion of coal in current production mines [4,5]. The CO concentration exceeded the limit at the 302 comprehensive mining working face of Da Shui Tou coal mine [6]. The CO concentration exceeded the limit in the corner of the working face of Mindong Mine. It was found that the CO originated from the original coal seam fugacity, the coal mining process and the natural fire of the coal left in the mining area [7]. The abnormal CO concentration is affected by various conditions such as the pore structure of the coal body, the coal mining environment and the degree of metamorphism. Lin [8] et al. analyzed the pore structure of tectonic and primary coal and found that the pore structure of tectonic coal is more complex. Yang [9] conducted crushing experiments on coal bodies under air environment and found that there was a correspondence between coal specific surface area and CO production. Zhang [10] studied the coal mining site and found that the instantaneous temperature of the cut-off teeth during coal mining could reach 600 °C, and the mechanical energy conversion would lead to the instantaneous oxidation of the

coal body by increasing the temperature to produce CO. Wang [11] et al. found that the CO produced during coal mining was generated by the oxidation reaction due to the fracture of coal molecules generating a large number of free radicals. Liu [12] et al. concluded that CO mainly originated from the free radicals generated by the breakage of functional groups and molecular chains caused by cannon discharge and coal cutting. Wang [13] suggested that the reactive groups on the coal surface play an intermediary role in the oxidation stage before combustion. Sun [14] et al. found carbon–oxygen-containing groups as oxidation intermediate functional groups for CO production at room temperature in coals with low degree of metamorphism. Ma [15] et al. studied three degradation degree coal samples and found that the sources of CO include mechanical crushing activated decarbonation, as well as coal surface free radical oxidation and coal oxygen complex reaction.

Most of the studies on CO sources by domestic and foreign scholars focus on mechanical crushing and warming oxidation, without considering the large error of detection methods and the low-temperature oxidation of the coal body. In this paper, we apply CO identification tube, programmed warming-gas chromatography experiments, low-temperature water bath experiments, liquid nitrogen adsorption experiments, thermogravimetric experiments and Fourier infrared spectroscopy experiments to analyze the phenomenon of low-temperature CO generation in coal body from both macroscopic and microscopic perspectives, which is important for mine fire prevention work.

2. Gas Chromatograph-CO Identification Tube Comparison Experiment

According to the past experience, we take the gas chromatograph detection results as the actual situation by default, but in the actual production process, the underground staff cannot use the gas chromatograph but use the CO identification tube, and the identification tube detection results and the results measured by the gas chromatograph have certain errors. In order to find the relationship between CO identification tube and gas and for chromatograph results to be closer to the actual situation, the raw coal sample was subjected to a programmed warming-gas chromatography experiment, in which the raw coal was crushed and sieved to obtain 80 g of 60–80 mesh coal sample, which was put into the sample tank of the warming furnace, and the gas introduced was compressed air with a gas flow rate of 100 mL/min. Moreover, the ramp-up stage was set as follows: room temperature to 30 °C set for 10 min and 30 °C held for 10 min, and the ramp-up rate to the maximum temperature of 150 °C was set as 0.6 °C/min. The gas was collected at 10 °C intervals, and the collected gas samples were subjected to gas chromatography experiments. At the same time, the gas sample obtained by the programmed temperature rise was detected using a CO identification tube. Then, 100 mL of a gas sample was extracted with a detector, and the gas sample was passed through the detector tube at a uniform rate for 200 s. The obtained results are shown in Figure 1.

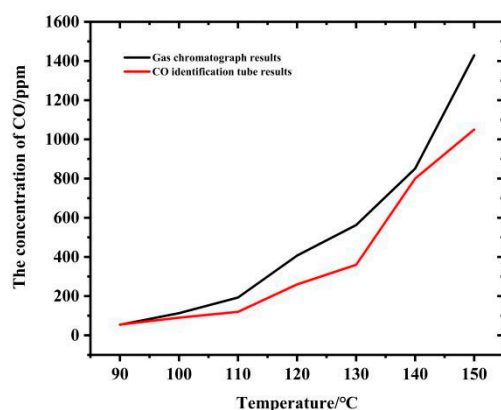


Figure 1. Programmed temperature rise—gas chromatography experiment and CO identification tube results.

From Figure 1, it can be seen that the CO concentration in the gas sample detected by the gas chromatograph gradually increases with the increase in temperature. The detection results of the two methods were significantly different, and their average relative error reached 125. Although there is a certain deviation between the data measured by the CO identification tube and the data measured by the gas chromatograph, the overall trend tends to be consistent. Therefore, the data measured by the two measurement methods can be fitted to obtain the correspondence between the two, so as to achieve the purpose of inferring the value measured by the gas chromatograph from the value measured by the CO identification tube, making it closer to the real value.

The fitting curve equation is as follows:

$$Y_g = 37.64e^{0.5334X} \quad (1)$$

$$R_g^2 = 0.9863 \quad (2)$$

$$Y_t = 31.128e^{0.5113X} \quad (3)$$

$$R_t^2 = 0.9875 \quad (4)$$

where:

Y_g —Results measured by meteorological chromatograph/ppm;

Y_t —Results measured by CO identification tube/ppm;

X —Temperature/°C;

R_g^2, R_t^2 —The correlation coefficient of the fitted curve.

The correlation coefficients of the fitted curves are within a reasonable range, so the fitting results can be considered as correct. The association of Equations (1) and (3) by Eq. So that the CO identification tube is the independent variable, the gas chromatograph detection results can be deduced:

$$Y_g = 37.64e^{1.043\ln\frac{Y_t}{31.128}} \quad (5)$$

3. Artificial Preparation and Experimental Analysis of Low Temperature Coal Oxide

3.1. Sampling and Preparation

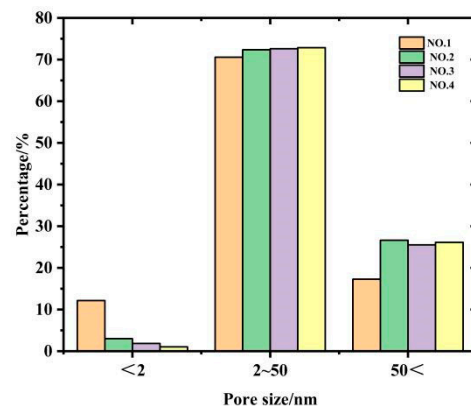
The coal samples collected in this experiment were taken from the 0291 coal seam of Tangshan Mine, 110 m from the duct entrance on the return airway side and 10 m from the inclination length, using a wind drill locomotive, withdrawing the drill after drilling 10 m into the coal seam and quickly loading the removed coal samples into 4 coal sample jars, then sealing the jars. The four retrieved coal samples were labeled as No. 1 to No. 4. The No. 1 coal sample canister was used as the control group without any treatment, and the No. 2 to No. 4 canisters were put into the constant temperature water bath for heating at 30 °C, 40 °C and 50 °C [16], respectively, for 24 h. Since the coal sample canisters needed to be sealed and the volume of the canisters was limited, the amount of gas inside the canisters was small, and the concentration of CO in canister No. 1 was low, so it was difficult to perform gas chromatography experiments. Therefore, the CO identification tube was used for testing.

3.2. Pore Size Analysis of Low Temperature Oxidized Coal

With the increase in temperature, the pores of the coal body develop, which shows the enhancement of the pore structure. The change in pore structure affects the ability of the coal body to adsorb gas [17], and the pore structure of the coal body is generally characterized by porosity, specific surface area, pore volume, average pore size, etc. To study the effect of the low-temperature environment on the change in the pore size distribution, low-temperature liquid nitrogen adsorption experiments were conducted on coal samples 1~4, and the results are shown in Table 1 and Figure 2.

Table 1. Pore size distribution.

Number	Specific Surface Area/(m ² /g)	Average Pore Size/nm	Hole Volume/(cm ³ /g)
1	2.179	11.381	0.004
2	2.755	12.231	0.006
3	4.039	13.100	0.008
4	4.523	14.035	0.009

**Figure 2.** Proportion of microporous, mesoporous and macropore for each coal sample.

As can be seen from Table 1, the specific surface area, average pore size and pore volume of the coal body showed an increasing trend with the increase in temperature.

As shown in Figure 2, the number of mesopores of the coal samples treated with water baths and heat increased, the number of macropores increased from 17% to about 26% and the number of micropores decreased from 12% to about 3% and showed a trend with temperature. Nanoscale pores are the main contributors to the specific surface area of coal bodies [18], and therefore, the increase in specific surface area also proves that the water bath plus heat treatment promotes the conversion of micropores to mesopores as well as macropores in the coal body; the increase in the average pore size and the increase in the pore volume indicate the increase in the number of macropores as well as mesopores. The change of pore size structure affects the CO adsorption capacity of the coal body: The larger the pore size and the greater the number of macropores, the stronger the CO adsorption capacity.

3.3. Analysis of CO Release Pattern of Low-Temperature Coal Oxide

A 100 mL gas sample was immediately taken from the retrieved tank No. 1, and the CO concentration in the gas sample was measured. The same method was used to extract the gas from canisters 1 to 4 for CO concentration detection after 24 h of heating in a water bath. The results are shown in Table 2.

Table 2. CO concentration of tanks 1~4.

Can No.	1	2	3	4
CO concentration/ppm	10	160	280	500

As can be seen from Table 2, the CO concentration of 10 ppm in tank 1 indicates the presence of primary or secondary CO in the coal sample. The gas sample was taken again after 24 h, and the CO concentration was still 10 ppm, indicating that the untreated coal sample No. 1 did not undergo any chemical change in the environment of the coal sample tank less than 30 °C. The analysis of the gas samples of coal sample tanks 2~4 heated by water bath at different temperatures showed that the CO concentration increased with the increase in the water bath temperature. Some of the CO is generated due to the increase in temperature, originally in the adsorbed state of CO into the free state, and another

part of CO is considered to be generated by the oxidation reaction of the coal body in the low-temperature environment [19]. Thermogravimetric experiments were conducted on the raw coal, and the experimental results are shown in Figure 3.

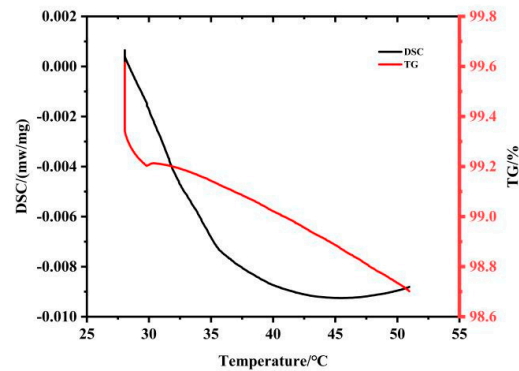


Figure 3. Thermal weight curve of raw coal sample.

As seen in Figure 3, the heat flow curve is always less than 0, showing a trend of first decreasing and then increasing. It means that under the low temperature condition of 30~50 °C, the coal body has been in the state of heat absorption. A temperature of 30~50 °C in the coal body mass shows a decreasing trend, and the increase in the coal body temperature makes the small amount of oxygen-containing functional groups, side chains and other smaller molecular structures in the coal crack and contact with oxygen to generate volatile gas [20]. This leads to the decrease in coal mass.

3.4. Low Temperature Coal Oxide CO Source Analysis

In order to more accurately analyze the source of CO in low-temperature environments, the effect of microstructural changes in the coal body was considered. The changes of the main functional groups in the coal body by water bath at different temperatures were investigated by infrared spectroscopy experiments, and the influence of temperature on the changes in the content of active functional groups in coal was analyzed using the infrared spectrograms of coal samples in tanks 1~4, i.e., raw coal, 30 °C, 40 °C and 50 °C water-bath-heated coal samples. The coal samples from jars 1 to 4 were taken out, crushed, sieved and dried under vacuum at 30 °C to obtain 5 mg of coal samples below 200 mesh by the KBr compression method (Coal sample powder was mixed with KBr powder in the ratio of 1:150 and poured into a bowl to grind and pressed into thin slices with a thickness of about 1 mm using a tablet press). The parameters of the experimental equipment were set as follows: The PoP scanning interval was 400–4000 cm^{-1} , the resolution was set to 4.0 cm^{-1} and the IR spectra of each sample were scanned 30 times. The IR spectra of the raw coal and the coal samples treated with different temperature water baths were extracted separately, as shown in Figure 4.

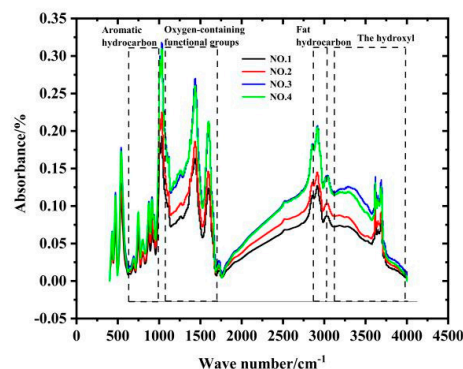


Figure 4. Infrared spectra of coal samples 1 to 4 after fitting treatment.

From Figure 4, since the coal samples were selected from the same coal seam, it can be seen that the absorbance peak positions of different coal samples basically correspond to the same. With the change in temperature, the intensity of the infrared absorption peaks of the coal samples at different wavelengths show obvious variability. Temperature changes lead to changes in the content of each functional group in the coal body. The wave number of aromatic hydrocarbon benzene ring substituents is basically in the range of 690~900 cm^{-1} , the C=C skeleton representative wave number is 1599~1604 cm^{-1} and the C-H skeleton representative wave number is 3030~3056 cm^{-1} . For oxygen-containing functional groups, the wave numbers are basically in the range of 1040~1790 cm^{-1} , including 1040~1220 cm^{-1} for the ether bond; 1700~1710 cm^{-1} for the carbonyl group of aldehydes, ketones and acids; 1770~1790 cm^{-1} for the carbonyl group of esters; and 1722~1758 cm^{-1} for the carboxyl group of esters. The wave numbers of methyl and methylene groups of aliphatic hydrocarbons are basically in the range of 2858~3040 cm^{-1} ; the wave numbers of hydroxyl groups are basically in the range of 3200~3697 cm^{-1} , which include intermolecularly joined hydrogen bonds, intramolecular hydrogen bonds and free hydroxyl groups.

Coal is a macromolecular substance composed of many functional groups, and the number of different kinds of functional groups determines the chemical properties of coal. In the original chromatogram, because the absorption bands of many functional groups contribute to the infrared spectrum, it is easy to produce the phenomenon of superposition of spectral peaks at a certain position, so the method of split-peak fitting is used to separate the overlapping peaks to obtain the area of characteristic absorption peaks. The area of the absorption peaks of the same functional group is integrated according to the peak position attribution of different functional groups to calculate the proportion of each functional group, as shown in the Table 3.

Table 3. Percentage of main functional groups in each coal sample.

Coal Sample Number	Aliphatic Hydrocarbons -CH ₂ /-CH ₃	Aromatic Hydrocarbon	Oxygen-Containing Functional Groups				
			-OH	C=O	-COOH	C-O	All
NO.1	24.26	12.75	41.48	0.33	0.46	20.61	62.99
NO.2	23.17	14.71	39.72	0.31	0.44	21.65	62.12
NO.3	22.65	11.96	42.90	0.37	0.53	21.59	65.39
NO.4	23.3	12.44	41.13	0.27	0.39	22.46	64.25

unit: %.

From Table 3, it can be seen that the proportion of aromatic hydrocarbon functional group content with the increase in water bath temperature generally shows a rising trend and then decreases. At around 30 °C, the number of aromatic hydrocarbons increases, while the number of other functional groups does not change significantly, so the proportion of aromatic hydrocarbons increases. At the 40~50 °C stage, although the number of aromatic hydrocarbons still increases but other functional groups also show a growing trend so their proportion decreases. The aliphatic hydrocarbon components and carbonyl groups play a major role in the low temperature oxidation process of coal [21]. The proportion of aliphatic hydrocarbons is the lowest compared with other temperatures at 40 °C, while the proportion of carbonyl groups is the highest. Aliphatic hydrocarbons are easy to oxidize with oxygen in the low-temperature environment to generate various oxygen-containing functional groups, including carbonyl group. The carbonyl group is slow to oxidize in this low-temperature environment, and the generation rate is larger than the decomposition rate. Therefore, as the proportion of carbonyl increases in the 50 °C environment, the decomposition rate accelerates, and the proportion begins to decline. With the increase in water bath temperature, the hydroxyl and carboxyl groups showed a trend of rising first and then falling, and the content of hydroxyl and carboxyl groups in No. 2 coal sample was almost unchanged compared with No. 1. It can be considered that the environment of 30 °C had almost no effect on hydroxyl and carboxyl groups. The proportion of hydroxyl and

carboxyl groups in coal sample No. 3 increased, the rise of carboxyl groups in it reached 20.5%, the generation of hydroxyl and carboxyl groups was greater than the decomposition amount and the oxidation of aliphatic hydrocarbons occurred in the 40 °C environment. The reaction generated a variety of peroxides. Peroxides are unstable and further oxidize to generate hydroxyl, carboxyl and other oxygen-containing functional groups. The 50 °C coal samples showed condensation and elimination of hydroxyl groups, and the decomposition rate of carboxyl groups was greater than the generation rate, and the content of both decreased [22]. The content of the ether bond increases continuously with the increase in the water bath heating temperature. It can be seen that in the coal samples in the water bath at different temperatures, there has been the generation of ether bonds, and the generation rate is greater than the rate of decomposition. Combined with the CO content in each coal sample tank, each functional group was analyzed one by one. A line graph of the CO concentration versus the absorption peak area value of each functional group was plotted, as shown in Figure 5.

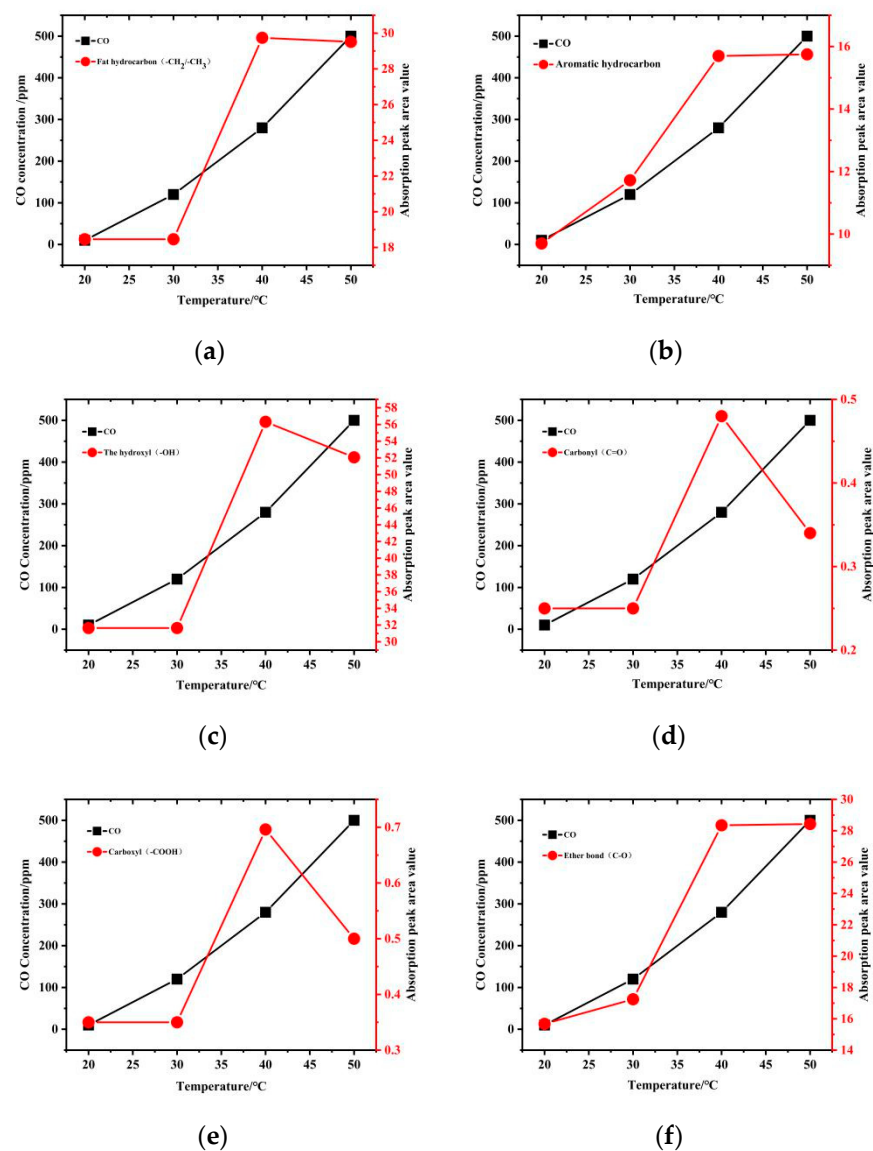
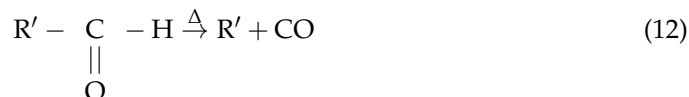
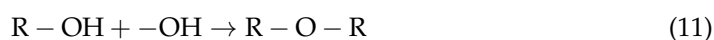
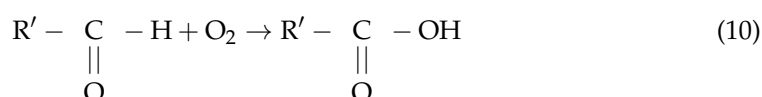
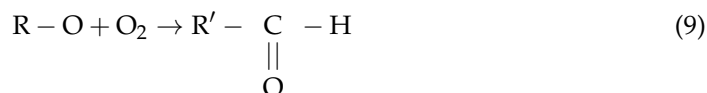
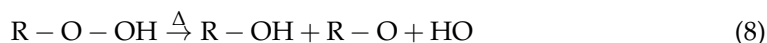
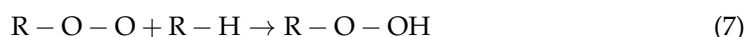
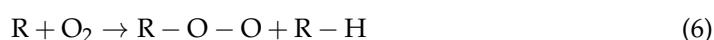


Figure 5. Line chart of CO concentration and absorption peak area of functional groups: (a) Aliphatic hydrocarbons, (b) Aromatic hydrocarbons, (c) Hydroxyl, (d) Carbonyl, (e) Carboxyl group, (f) Ether bond.

From Figure 5, during the heating process in the water bath at 30 °C, there is an increase in aromatic hydrocarbons (C-H), and the reaction activity of aliphatic hydrocarbon components in coal, especially the α -position methylene component connected with it, is the highest. In addition, chemisorption occurs to react with oxygen to produce aromatic hydrocarbons (C-H) and various peroxides [23], as shown in reaction Equation (6). During the heating of the water bath at 40 °C, the oxygen-containing functional groups, including hydroxyl, carbonyl and carboxyl groups, increase substantially. The peroxides produced by the oxidation reaction of the coal body during this process react with aromatic hydrocarbons (C-H) to produce hydrogen peroxide complexes, as shown in reaction (7). The hydrogen peroxide complex is further oxidized with increasing temperature to produce alcohols, hydrogen radicals and oxygenated radicals, as shown in reaction (8). The oxygen-containing radicals are further oxidized to form carbonyl [24] groups, as shown in reaction Equation (9). The carbonyl group in turn reacts with oxygen to form carboxyl group as shown in reaction Equation (10). As the temperature increases, the ether bonding continues to increase. After the decomposition of hydroperoxides into alcohols, oxygen-containing radicals and hydrogen radicals, the generated alcohols are further oxidized to generate unstable carbon–oxygen intermediates, which contain carbonyl groups, and the alcohols also react with hydroxyl groups to generate ether bonds. A similar reaction process exists for coal samples 2~4, as shown in reaction (11). Starting from coal sample No. 2, the CO content detected in the coal sample tank increased with the increase in the water bath temperature, and the CO production originated from the thermal decomposition of the carbonyl group in the water bath environment [25], as shown in reaction Equation (12). The carbonyl-containing radicals and oxygen-containing radicals generated during the oxidation of coal all accelerate the reaction rate of the coal spontaneous combustion system.



4. Preferred Natural Fire Predictor for Tangshan Mine

Since CO will be produced by the coal body at low temperatures, the CO concentration cannot be used as an indicator gas for the prediction of coal spontaneous combustion firing in the media. Different indicator gases are set for different temperature stages for CO, CH₄, C₂H₆, O₂/(CO+CO₂), CO₂/CO, CH₄/CO and other indicators were subjected to gray correlation analysis to determine the optimal indicators at each temperature stage and eliminate the effects of abnormal CO influx. The correlations of each indicator at different temperature stages were obtained as shown in Table 4.

Table 4. Correlation ranking of each index at different temperature stages.

Temperature Stage/°C	Gray Correlation Ranking					
	CO	CH ₄	C ₂ H ₆	O ₂ /(CO+CO ₂)	CO ₂ /CO	CH ₄ /CO
30~80				1		
90~180	2	1		3	5	4
180~240	5	3	6	4	1	2

The correlations of the indicators for the Tangshan mine were ranked as shown in Table 4. Since the coal body is known to produce CO in the low-temperature stage, CO is not considered as an indicator gas in the low-temperature stage in order to eliminate the effect of abnormal CO outgassing. O₂/(CO+CO₂) is selected as the index of spontaneous combustion in the low-temperature stage. The generation of CO, CH₄, C₂H₆ and other gases increases after the temperature of coal body reaches above 90 °C, which indicates that the coal molecules obtain a lot of energy at this stage, the molecular structure changes, and the chemical bonds of each reactive group gradually break, generating a large number of free radicals and peroxide complexes, which combine with oxygen to generate CO and gaseous hydrocarbon gases. In the stage of 90~180 °C, CH₄ has the highest correlation, which indicates that CH₄ as an indicator gas is the closest to the natural oxidation temperature change dynamics of coal and has the best prediction effect, followed by CO. In the stage of 180~240 °C, the CO₂/CO indicator is the preferred indicator, and CH₄/CO can be used as the second prediction indicator.

5. Conclusions

(1) The CO identification tube test results and gas chromatograph test results were derived separately from the fitting formula, and the correlation coefficients proved that the fitting results were accurate, and the mathematical formula with the CO identification tube test results as the independent variable and the gas chromatograph test results as the dependent variable was derived from the joint formula, which effectively reduced the CO identification tube test errors.

(2) With the increase in the water bath temperature, the specific surface area, average pore size and pore volume of the coal body showed an increasing trend, the number of micropores decreased, and the number of macropores and mesopores increased; the coal sample in this environment was in the state of heat absorption before oxidation, accompanied by the decrease in the coal body mass indicating the generation of CO.

(3) The microstructure of the coal body changes in the low temperature water bath heating environment. In the 30 °C environment, aliphatic hydrocarbons are more active and oxygen reaction to generate aromatic hydrocarbons (C-H) and various peroxides, resulting in an increase in the content of aromatic hydrocarbons (C-H). In the 40 °C water bath heating, the content of oxygen-containing functional groups increased; the generation process is as follows: peroxide and aromatic hydrocarbons (C-H) reaction to generate hydrogen peroxide complexes and hydrogen peroxide; the hydrogen peroxide complex is decomposed by heat to produce alcohol, hydrogen radical and oxygen radical, which are further oxidized to produce carbonyl group and oxidized to produce carboxyl group; the alcohol reacts with the hydroxyl group to form an ether bond, which is generated throughout each stage of the water bath heating. CO is derived from the thermal decomposition of the carbonyl group.

(4) Using the grey correlation analysis method to optimize the mine natural fire prediction index, it was determined the stage of 30~80 °C O₂/(CO+CO₂) would be used as the prediction index. In the stage of 90~180 °C, CH₄ is the first predictor and CO is the second predictor. In the stage of 180~240 °C, CO₂/CO is the first predictor and CH₄/CO is the second predictor.

Author Contributions: Conceptualization, J.Z.; methodology, G.R.; software, G.R.; validation, J.Z. and G.R.; formal analysis, J.Z. and G.R.; investigation, J.C.; resources, J.Z. and G.R.; data curation, G.R.; writing—original draft preparation, G.R.; writing—review and editing, J.Z.; visualization, G.R.; supervision, J.Z.; project administration, J.Z.; funding acquisition, J.Z. All authors have read and agreed to the published version of the manuscript.

Funding: This research received no external funding.

Institutional Review Board Statement: Not applicable.

Informed Consent Statement: Not applicable.

Data Availability Statement: Not applicable.

Conflicts of Interest: The authors declare no conflict of interest.

References

1. Zheng, X.; Hui, S.; Wen, H.; Guo, J. Research progress on mechanism and prevention and control technology of mine fire. *Saf. Coal Mines* **2017**, *48*, 5.
2. Yuan, L. Research on the development strategy of coal mine safety in China. *China Coal* **2021**, *47*, 1–6. [[CrossRef](#)]
3. Wang, H. Study on the Mechanism of Primary CO Generation in Coal Seams and the Characteristics of Adsorption and Dispersion. Ph.D. Thesis, China University of Mining and Technology, Beijing, China, 2015.
4. Jia, H.; Yu, G.; Xu, Y. Analysis on the genetic type and mechanism identification of carbon monoxide in the coalmine. *J. China Coal Soc.* **2013**, *38*, 1812–1818.
5. Liang, Y.; Zhang, J.; Wang, L.; Luo, H.; Ren, T. Forecasting spontaneous combustion of coal in underground coal mines by index gases: A review. *J. Loss Prev. Process Ind.* **2019**, *57*, 208–222. [[CrossRef](#)]
6. Shao, S.; Su, X.; Zhao, L.; Tang, Y.; Jin, S. Analysis and management of CO sources in the mining void area of west 302 header working face of Dashuitou coal mine. *Mod. Min.* **2019**, *35*, 243–245.
7. Huang, G.; Gao, G.; Li, S. Analysis of CO sources in aged lignite comprehensive working face and research on treatment technology. *Energy Environ. Prot.* **2020**, *42*, 67–70. [[CrossRef](#)]
8. Lin, H.; Tian, S.; Jiao, A.; Ma, R.; Xu, S. Pore characteristics and fractal shape of tectonic and primary structural coal in Qianbei region, Guizhou. *Sci. Technol. Eng.* **2021**, *21*, 14451–14458.
9. Peng, Y.; Zhuang, H. Source analysis of CO in working face upper corner of xichuan coal mine. *Coal Eng.* **2018**, *50*, 100–104.
10. Zhang, H. CO gas source analysis of W1714 Fully mechanized mining face. *Min. Saf. Environ. Prot.* **2010**, *37*, 99–100.
11. Wang, X.; Wu, J.; Wu, Y. Source analysis and overrun measures of CO at working face in shendong mining area. *Saf. Coal Mines* **2013**, *44*, 132–134.
12. Liu, P.; Huang, H.; Zeng, J. CO source analysis and establishment of spontaneous combustion prediction system in Fully mechanized Caving Face of Sima Mine. *Min. Saf. Environ. Prot.* **2009**, *36*, 61–63.
13. Wang, H. Fourier infrared spectroscopy analysis of the chemical structure of coal surface with different disposal methods. *Coal Mine Saf.* **2017**, *48*, 177–181. [[CrossRef](#)]
14. Sun, W.; Shi, J.; Zhang, H.; Zhao, Y.; Wang, K.; Chen, Q. Analysis of oxidation intermediate functional groups for CO generation during spontaneous combustion of low metamorphic coal species. *Coal Mine Saf.* **2021**, *52*, 217–221. [[CrossRef](#)]
15. Ma, L.; Wei, Z.; Zou, L.; Wei, G.; Liu, X. Experimental test and analysis of CO gas source during coal seam mining. *J. China Univ. Min. Technol.* **2021**, *50*, 214–219.
16. Deng, J.; Xiao, Y.; Li, Q.; Lu, J.; Wen, H. Experimental studies of spontaneous combustion and anaerobic cooling of coal. *Fuel* **2015**, *157*, 261–269. [[CrossRef](#)]
17. Li, X.; Shao, Y.; Zhu, Y.; Zou, M.; Xu, X. Pore fractal characteristics of coal rocks based on low-temperature liquid nitrogen adsorption. *Sci. Technol. Eng.* **2022**, *22*, 65–70.
18. Yan, J.; Bo, Z.; Yang, Y. Effect of nanoscale pores on the gas adsorption capacity of tectonic coal. *Chin. J. Saf. Sci.* **2018**, *28*, 131–136. [[CrossRef](#)]
19. Onifade, M.; Genc, B. Spontaneous combustion liability of coal and coal-shale: A review of prediction methods. *Int. J. Coal Sci. Technol.* **2019**, *6*, 151–168. [[CrossRef](#)]
20. Zhu, L.; Zhou, Y.; Wang, X.; Deng, Y. Study on the mechanism and prediction of CO anomalous gushing in igneous rock-influenced areas. *Coal Sci. Technol.* **2019**, *47*, 152–157. [[CrossRef](#)]
21. Zhong, X.; Kan, L.; Xin, H.; Qin, B.; Dou, G. Thermal effects and active group differentiation of low-rank coal during low-temperature oxidation under vacuum drying after water immersion. *Fuel* **2019**, *236*, 1204–1212. [[CrossRef](#)]
22. Niu, Z.; Liu, G.; Yin, H.; Wu, D.; Zhou, C. Investigation of mechanism and kinetics of non-isothermal low temperature pyrolysis of perhydrous bituminous coal by in-situ FTIR. *Fuel* **2016**, *172*, 1–10. [[CrossRef](#)]
23. Xu, T. Heat effect of the oxygen-containing functional groups in coal during spontaneous combustion processes. *Adv. Powder Technol.* **2017**, *28*, 1841–1848. [[CrossRef](#)]

-
24. Ma, L.; Wang, D.; Kang, W.; Xin, H.; Dou, G. Comparison of the staged inhibitory effects of two ionic liquids on spontaneous combustion of coal based on in situ FTIR and micro-calorimetric kinetic analyses. *Process Saf. Environ. Prot.* **2019**, *121*, 326–337. [[CrossRef](#)]
 25. Li, J.; Li, Z.; Yang, Y.; Niu, J.; Meng, Q. Room temperature oxidation of active sites in coal under multi-factor conditions and corresponding reaction mechanism. *Fuel* **2019**, *256*, 115901. [[CrossRef](#)]